

# Poly(lactide) Nanofibers Produced by a Melt-Electrospinning System with a Laser Melting Device

Nobuo Ogata, Shinji Yamaguchi, Naoki Shimada, Gang Lu, Toshiharu Iwata, Koji Nakane, Takashi Ogihara

Department of Materials Science and Engineering, University of Fukui, Fukui 910-8507, Japan

Received 16 June 2006; accepted 9 November 2006

DOI 10.1002/app.25782

Published online in Wiley InterScience (www.interscience.wiley.com).

**ABSTRACT:** A new melt-electrospinning system equipped with a CO<sub>2</sub>-laser melting device was developed. Rod-like samples were prepared from poly(lactide) pellets, and then fibers were produced from the samples using the new system. The effects of producing conditions on the fiber diameter were investigated. Furthermore, the physical properties of the fibers were investigated. The following conclusions were obtained: (i) in a special case, fibers having an average fiber diameter smaller than 1 μm could be obtained using the system developed; (ii) the fiber diameter

could be decreased with increased laser output power, but the physical properties of the fibers such as the melting point and the molecular weight were decreased; and (iii) the electrospun fibers exhibited an amorphous state, and the annealed fibers exhibited an isotropic crystal orientation. © 2007 Wiley Periodicals, Inc. *J Appl Polym Sci* 104: 1640–1645, 2007

**Key words:** melt-electrospinning; poly(lactide); laser melting

## INTRODUCTION

Recently, various engineering fields have been paying a great deal of attention to nanoscale materials. In particular, nanofibers have been desired and developed in the fiber industry. The fibers are potentially useful in a variety of engineering applications in which a large surface area and fibrous structure are demanded.<sup>1–3</sup> Electrospinning is a simple technique for the production of nanofibers, and is classified into two kinds of methods: solvent-based electrospinning methods (S-ESP) and melt-based electrospinning methods (M-ESP). Although S-ESPs have solvent recycling issues and low productivity, studies using these methods abound because setup is inexpensive and simple. Since no solvent is used for melt-electrospinning, M-ESP eliminates the issues related to solvents. In other words, M-ESP is thought to be a more eco-friendly, versatile, and low-cost production method.

Despite these many potential benefits, the work on M-ESP is still relatively scarce.<sup>4,5</sup> The reasons why M-ESP is not widely used are as follows: (i) it is thought that the fibers with smaller fiber diameters are produced by S-ESP because the solvent in the spinning liquid is vaporized during the fiber formation process; (ii) the viscosity of molten polymer is

high compared with that of polymer solution, so that, given the mechanism for fiber formation, nanofibers seem less likely to form<sup>1</sup>; (iii) the system for applying high voltage to the molten polymer is difficult to manufacture because of electric discharge problems; and (iv) there are scarcely any successful examples of using M-ESP for obtaining nanofibers.

It is known that high-modulus fibers and fine-diameter fibers can be obtained by the irradiation of a CO<sub>2</sub> laser beam to thermoplastic polymers being formed into fibers beneath the spinneret.<sup>6,7</sup> However, laser beam heating is not applied to the melt-electrospinning process. The laser beam heating prevents the electric discharge problems of the conventional melt-electrospinning because heating is performed from a distance. Therefore, the melt-electrospinning systems with laser heating device should be simpler than those developed by other researchers.<sup>4,8</sup> Polymers having relatively high melting points, such as poly(lactide) (PLA), poly(ethylene terephthalate), and thermotropic liquid-crystalline polymers, can be easily electrospun using the system because their melts can be produced only by increasing laser output power. In the case of the conventional melt-electrospinning process, the molten polymer is exposed to long-term thermal degradation. However, in the case of the melt-electrospinning process with a laser heating device, the polymer can be locally and instantaneously melted so that the molten polymer is not exposed to long-term thermal degradation and thermal dispersion is minimized. Thus, a melt-electrospinning system with a laser heating device seems to have several advantages.

Correspondence to: N. Ogata (ogata@matse.fukui-u.ac.jp).  
Contract grant sponsor: Kuraray Co., Ltd.

PLA is an eco-friendly and biodegradable polymer. That is, this polymer is synthesized from natural resources, hydrolyzed, degraded by microbes, and finally changed to carbon dioxide and water under natural circumstances. Furthermore, PLA is innocuous and biocompatible with human tissues. Therefore, the polymer has been used not only in the packaging field but also in the field of orthopedic surgery.<sup>9,10</sup> It is known that nanofiber mats made from PLA and its copolymers can be used as scaffolds for cell growth.<sup>11</sup> The nanofibers and nanoscale voids formed by the assembly of fibers are favorable for cell growth. Several investigations for producing PLA nanofiber scaffolds have been performed using S-ESP; the solvents generally used for S-ESP of PLA are toxic chloroform, chloromethane, and *N,N*-dimethyl formamide.<sup>12</sup> Since the solvents are vaporized during S-ESP process, solvent recovery equipment is necessary. Furthermore, the residual solvent must be thoroughly removed from the nanofiber mats before they are used as a scaffold for cell growth. It is clear that PLA nanofiber mats produced using S-ESP have problems related to solvents. However, PLA nanofiber mats produced using M-ESP avoid such problems.

In this work, a new electrospinning system equipped with a laser melting device has been developed, and PLA has been electrospun using the system. The effects of production conditions on the diameter of the fibers have been investigated. Furthermore, the physical properties of the fibers have been investigated.

## EXPERIMENTAL

### Materials

Two types of pellet-like poly(lactide) (PLA; Cargill Dow, #6200D and #6251D) were supplied by KURARAY (Osaka, Japan) used for testing samples. The characterization of these pellets is as follows: #6200D; the melt flow index, MFI (measuring conditions: 210°C, applied load 21.6N) = 22.3 (g/min),  $D$  (%) = 1.8,  $L$  (%) = 98.2,  $T_m$  = 171°C, and #6251D; MFI (measuring conditions: 210°C, applied load 21.6N) = 76.9 (g/min),  $D$  (%) = 1.4,  $L$  (%) = 98.6, and  $T_m$  = 170.7°C. It should be noted that the difference in MFI values between the two samples is large.

Rod-like samples of *ca.* 0.5 mm in diameter were made from the melt of these pellets using a Shimadzu Flow Tester CFT-500; the melting temperature was 170°C and the applied stress was from 1 to 7 MPa. The rod-like samples were provided for the melt-electrospinning tests.

### Melt-electrospinning system

Figure 1 shows a schematic diagram of the melt-electrospinning system developed in this work. A rod-like

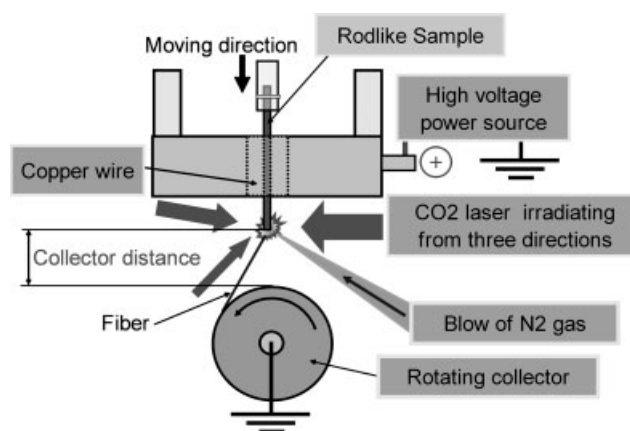


**Figure 1** Schematic diagram of the melt-electrospinning system developed in this work.

PLA sample was fed to the laser melting zone at a rate of 2–4 mm/s. One end of the rod was locally melted with an Onizca PIN-20R laser apparatus (Tokyo, Japan); the wave length was 10.6  $\mu\text{m}$ , the diameter of the laser spot was 5 mm, and the maximum power of the laser was 35 W. A high voltage was applied to the end of the rod through bulky copper wires from a black-stained aluminum electrode. To avoid burning of the rod-like samples during the laser heating,  $\text{N}_2$  gas was blown onto the laser-irradiated part. A grounded rotating disk was used to collect the fibers.

Figure 2 shows a schematic plan view of the laser irradiating beams. To melt the rod-like sample homogeneously, the end of the rod was irradiated by the laser beams from three directions.

### Melt-electrospinning conditions

A voltage at a height just before an electric discharge appeared was applied between the molten polymer and the grounded collector, and its maximum value was 41 kV; the voltage will be denoted as  $H_v$ . The end of the rod was irradiated by three laser beams; the maximum output power was 25 W and the power will be denoted as  $L_p$ . The molten end-to-collector distance was 20 mm unless otherwise noted; the distance will be denoted as the collector distance or  $C_d$  (Fig. 1). The peripheral velocity of the rotating disk was 1 m/s. Using these conditions, fibers were produced from the rod-like PLA. Although it was expected that many fibers would be simultaneously formed from a rod, it was found that only a single fiber was continuously formed from a rod during the melt-electrospinning process.

### Characterization of fibers

The morphology of the electrospun PLA fibers was examined by a Hitachi S-2300 scanning electron

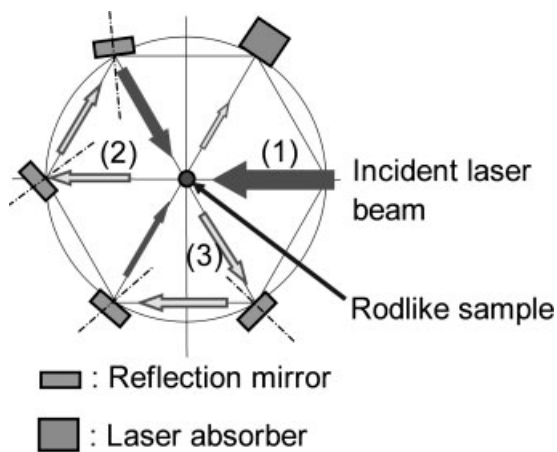


**Figure 2** Schematic plan view of laser irradiation beams.

microscope (SEM). The average and standard deviation of the fiber diameter were determined from 10 measurements of fibers obtained at each spinning condition; the average diameter and its standard deviation will be referred to as  $D$  and  $\sigma$ , respectively. The number of fibers for the evaluation of the average fiber diameter should be large. It was

observed that only a single fiber was continuously produced from a rod, and, therefore, the distribution of fiber diameter was narrow. From this reason, we determined that 10 measurements of fibers were enough to obtain the average diameter and standard deviation.

The molecular weight distribution and the number-average molecular weight of the fibers were evaluated in chloroform at 40°C with a Tosoh gel permeation chromatography (GPC) system (HLC-8220GPC); three TSK(HM-N) gel columns were used and the measured molecular weights were calculated by the universal calibration method using nine polystyrene reference materials. The fiber samples (5 mg) were dissolved in 5 mL of chloroform. After the elimination of insoluble matter by filtration, 20  $\mu$ L of the solution was injected into the GPC system. Using this system, the molecular weight distribution and the number-average molecular weight  $M_n$  were measured.

The thermal behavior of the fibers was measured with a Shimadzu DSC60 differential scanning calorimeter at a heating scan rate of 10°C/min.

To evaluate the crystal orientation of the fibers, aligned PLA fibers were heat-treated with fixed ends

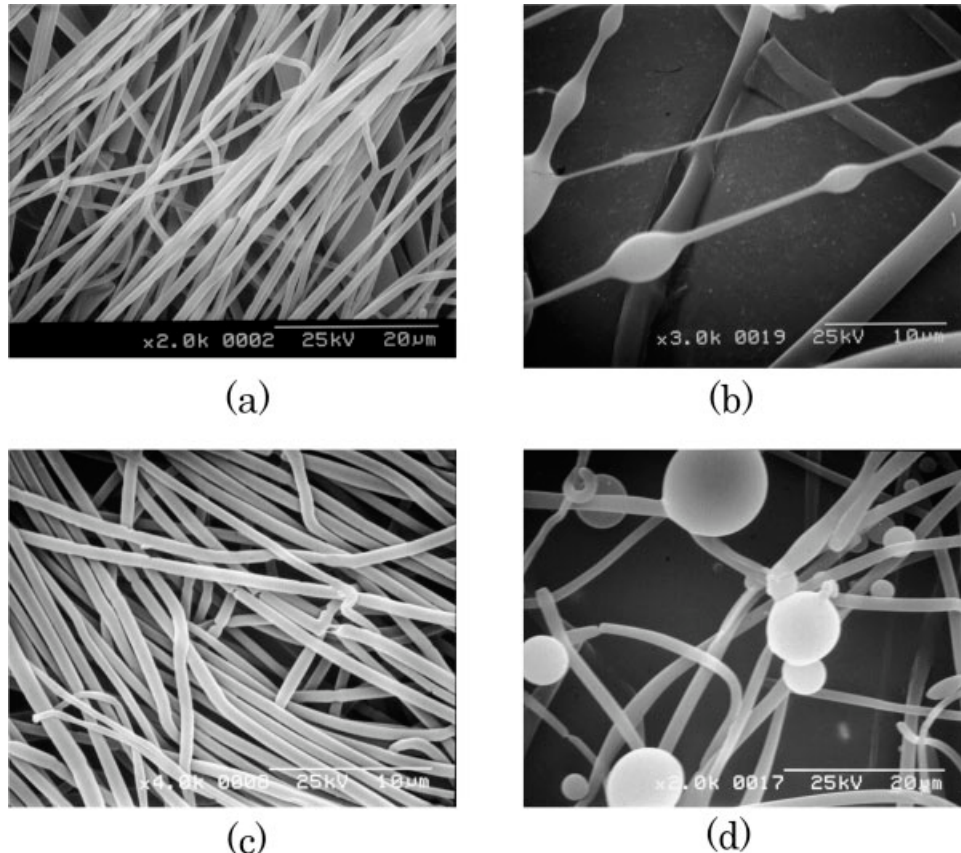


**Figure 3** SEM images of PLA fibers: (a) sample #6200D,  $D = 804$  nm,  $\sigma = 171$  nm,  $H_v = 30$  kV,  $L_p = 17$  W; (b) sample #6200D,  $H_v = 26$  kV,  $L_p = 22$  W; (c) sample #6251D,  $D = 712$  nm,  $\sigma = 167$  nm,  $H_v = 26$  kV,  $L_p = 13$  W; and (d) sample #6251D,  $H_v = 26$  kV,  $L_p = 21$  W.

at 100°C in air for 1 h. X-ray diffraction photographs of the annealed fibers were obtained with a Toshiba D-3 apparatus using Cu K $\alpha$  radiation. X-ray diffraction (XRD) curves of the annealed fibers were also obtained with a Rigaku RINT2000 apparatus using Cu K $\alpha$  radiation.

## RESULTS AND DISCUSSION

### Effect of processing conditions on fiber diameter

Figure 3 shows typical examples of the fibers produced using the system developed in this work. It can be seen that the fibers with a nanoscale diameter are formed. A branched fiber with a smaller diameter can be seen in Figure 3(b). The appearance of the branched fiber means that a side jet would be created from the molten jet during the application of high laser output power. Moreover, particles and fibers having beads can be seen [Fig. 3(d)]. These shapes were usually observed in the samples produced with a conventional S-ESP in which a polymer solution with low viscosity was used. Therefore, it seems that the actual melt viscosity during our

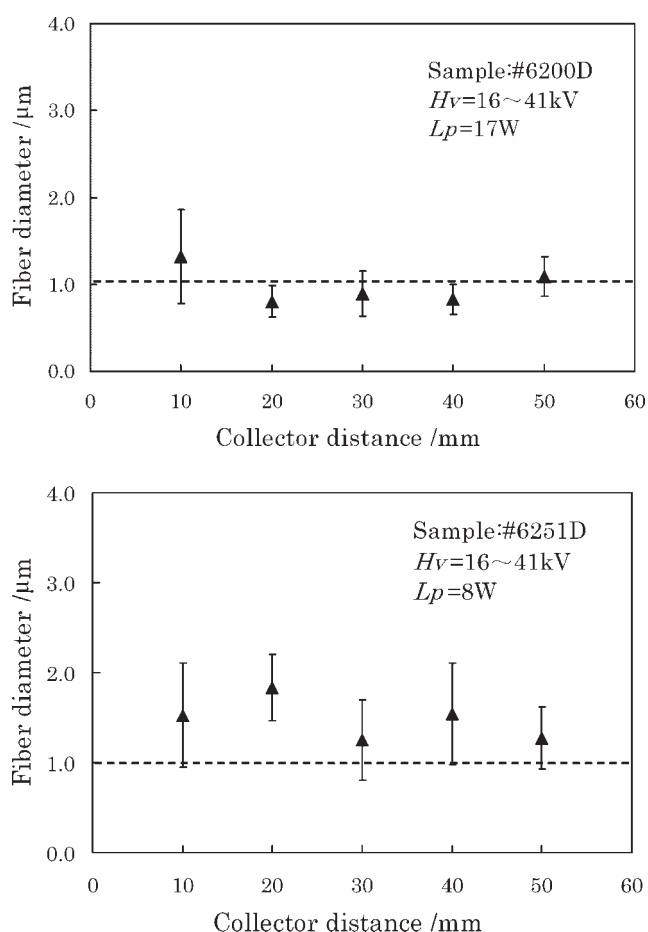


**Figure 4** Effect of molten end-to-collector distance,  $C_d$ , on the diameter of electrospun PLA fibers.

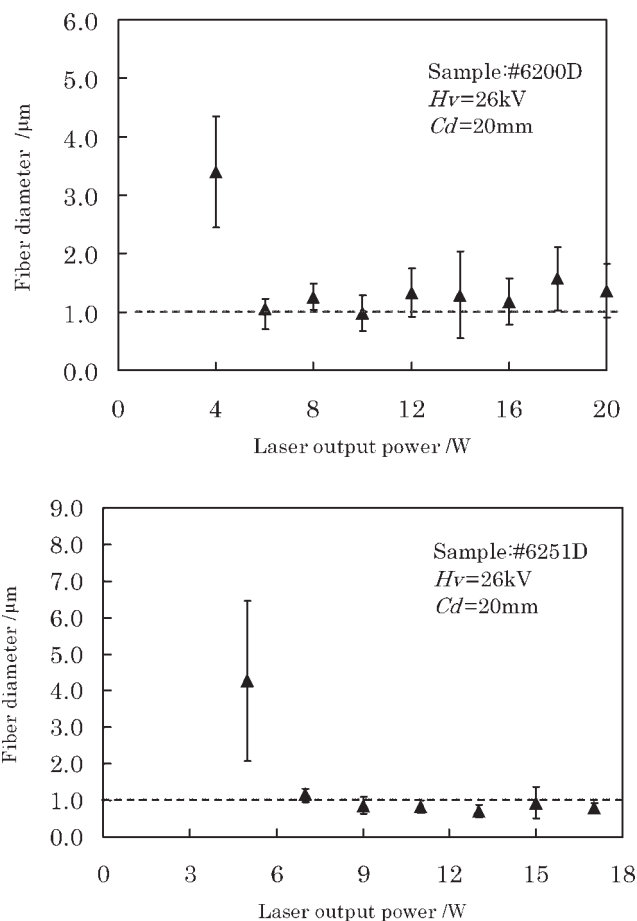


**Figure 5** Effects of laser output power on the diameter of electrospun PLA fibers.

melt-electrospinning process would be markedly low. From the photographs exhibiting fibers only, the average and standard deviation of the diameter of the fibers obtained for each producing condition were evaluated.

Figure 4 shows the effect of the collector distance,  $C_d$ , on the fiber diameter. It can be seen that the fiber diameter is almost independent of  $C_d$ . This result may be attributed to that the fiber diameter is influenced by the electric field strength.

Figure 5 shows the effect of laser output power on the fiber diameter. The diameter is large at a low laser output power, but decreases and then becomes constant with increasing laser output power. It seems that there is a lower limitation of the average fiber diameter. The diameter of fibers made from the high-MFI sample (#6251D) seems to be slightly smaller than that made from the low-MFI sample (#6200D). This result means that the fiber diameter is influenced by the value of MFI to some extent. It is apparent that the melt viscosity decreases with increasing laser output power. If it is assumed that the viscosity influences strongly the fiber diameter, then the fiber diameter would decrease monotonously with increasing laser output power. However,

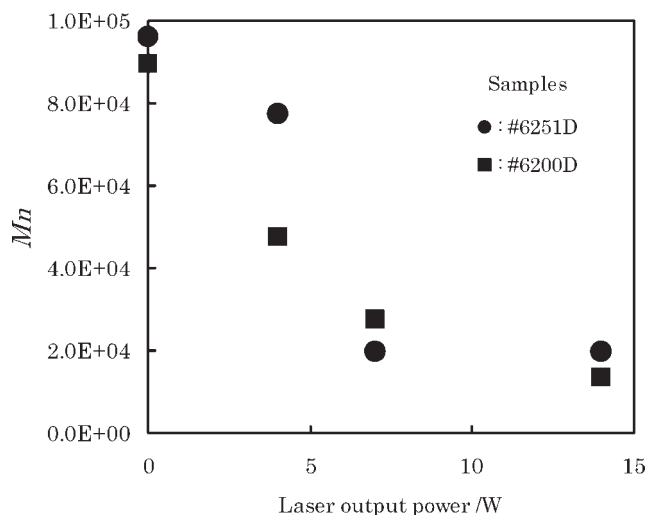


**Figure 6** Effect of laser output power on the number-average molecular weight ( $M_n$ ) of electrospun PLA fibers.

the experimental data do not support this idea. Therefore, it is concluded that the fiber diameter is not determined only by the melt viscosity, especially when the fiber having a diameter smaller than  $1\ \mu\text{m}$  was produced. When the laser output power greater than 20 W was applied, the fiber formation was unstable; the fibers were obtained from a mixture of particles, and were formed with the gas generation. This gas may be produced by the residue of thermal degradation of the PLA.

Finally, it should be noted that the fibers having an average diameter smaller than  $1\ \mu\text{m}$  can be produced using our melt-electrospinning system.

### Physical properties of the fibers

Figure 6 shows the effect of the laser output power on the number-average molecular weight  $M_n$  of the electrospun PLA fibers. The value of  $M_n$  decreases exponentially with increased laser output power, irrespective of the samples used. The decrease suggests that the laser melting induces molecular scission, which deteriorates the mechanical properties of the fibers; the laser heating induces significantly the scission of the ester bonds in PLA. It is noted that the decrease in the fiber diameter is accompanied with the increase in the thermal degradation. Therefore, the nanofibers made by laser irradiation are able to use not as strong tension members but as functional materials.

In the following discussion, only the data obtained from the experiments performed on #6251D fibers will be shown, because a similar result was obtained from those performed on #6200D fibers. Figure 7 shows the thermal behavior of the PLA nanofibers. Each sample shows an exothermal peak at about  $90^\circ\text{C}$ . The crystallization temperature increases slightly

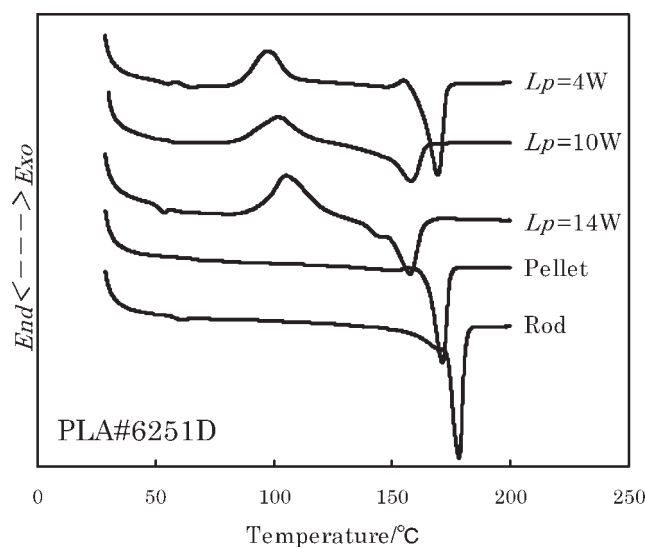


**Figure 7** Effect of laser output power on DSC curves of electrospun PLA (#6251D) fibers.

with increased laser output power; this result is unexpected because the molecular weight decreases with increased power and its decrease is thought to decrease the crystallization temperature. Regardless, the appearance of an exothermal peak means that the fibers are quickly quenched during the fiber formation process. It should be noted that the melting point decreases with increased laser output power. The size of the crystallites seems to become smaller with increasing laser output power; the decrease in the crystal size may be caused by the scission of the molecule.

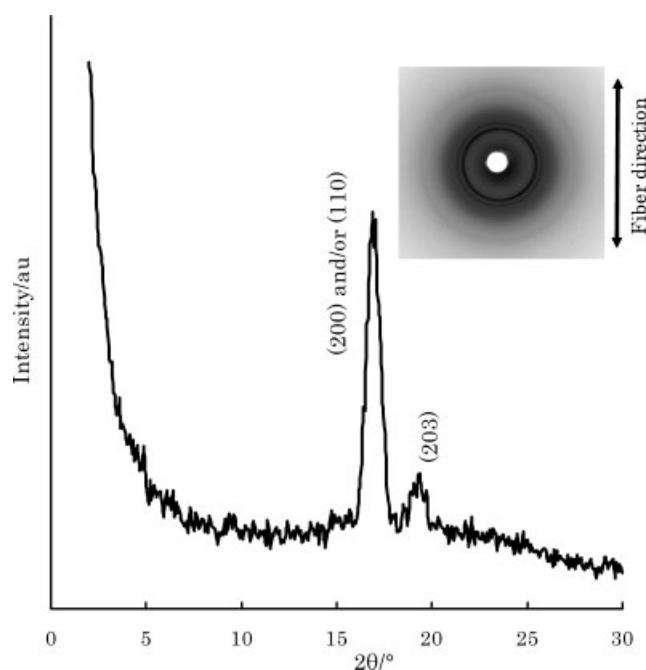


**Figure 8** X-ray photograph and XRD curve of PLA (#6251D) electrospun fibers.

Figure 8 shows X-ray photograph and the X-ray diffraction (XRD) curve of the annealed PLA nanofibers. Although the fibers were aligned in meridian, a strong intensity maximum ring can be seen. This pattern implies that the crystal orientation does not take place along the fiber direction. It is known that crystal orientation along the fiber direction is necessary for producing high-strength fibers, and the orientation can be obtained by drawing the fibers; drawing also makes the fiber diameter smaller. Therefore, increasing peripheral velocity of the rotating disk would be favorable for producing high-strength PLA nanofibers. The diffraction curve of PLA fibers exhibits a very strong reflection at  $2\theta = 17.1^\circ$  because of the diffraction between the (200) and/or (110) planes and another reflection peak at  $2\theta = 19.5^\circ$  occurring from the (203) plane.<sup>13,14</sup> The profile indicates that orthorhombic PLA crystals are formed in the annealing process of nanofibers.

### CONCLUSIONS

A melt-electrospinning system equipped with a laser melting device was developed and, using the system, PLA fibers produced. Furthermore, their morphologies and physical properties were investigated. The following conclusions were obtained:

1. The fibers having an average fiber diameter smaller than  $1\ \mu\text{m}$  can be produced in a special case.
2. The diameter of the fibers decreased with increased laser output power to some extent, although the

molecular weight and melting point of the fibers decreased by laser heating.

3. Amorphous fibers can be electrospun, and their annealed fibers showed an isotropic crystal orientation.

### References

1. Huang, Z.-M.; Zhang, Y.-Z.; Kotaki, M.; Ramakrishna, S. *Comp Sci Tech* 2003, 63, 2223.
2. Chronakis, I. S. *J Mater Process Tech* 2005, 167, 283.
3. Nasir, M.; Matsumoto, H.; Danno, T.; Minagawa, M.; Irisawa, T.; Shioya, M.; Tanioka, A. *J Polym Sci Part B: Polym Phys* 2006, 44, 779.
4. Lyons, J.; Li, C.; Ko, F. *Polymer* 2004, 45, 7597.
5. Reneker, D. H.; Chun, I. *Nanotechnology* 1996, 7, 216.
6. Nakata, K.; Ohkoshi, Y.; Gotoh, Y.; Nagura, M.; Funatsu, Y.; Kikutani, T. *SEN'I GAKKAISHI* 2004, 60, 352.
7. Yamaguchi, T.; Komoriyama, K.; Ohkoshi, Y.; Urakawa, H.; Gotoh, Y.; Terasawa, N.; Nagura, M.; Kajiwara, K. *J Polym Sci Part B: Polym Phys* 2005, 43, 1090.
8. Warner, L. S.; Ugbohue, S.; Jaffe, M.; Patra, P. National Textile Center, FY2005 New Project Proposal, No. F05-MD01, 2005.
9. Maurus, P. B.; Kaeding, C. C. *Operative Tech Sports Med* 2004, 12, 158.
10. Neuenschwander, S.; Hoerstrup, S. P. *Transplant Immunol* 2004, 12, 359.
11. Kim, K.; Yu, M.; Zong, X.; Chiu, J.; Fang, D.; Seo, Y. S.; Hsiao, B. S.; Chu, B.; Hadjiargyrou, M. *Biomaterials* 2003, 24, 4977.
12. Miyoshi, T.; Kobayashi, N.; Washimi, Y.; Minemura, H. *Jpn. Pat. P2003-90025* (2003).
13. Eling, B.; Gogolewski, S.; Pennings, A. J. *Polymer* 1982, 23, 1587.
14. Hoogsteen, W.; Postema, A. R.; Pennings, A. J.; TenBrinke, G.; Zugenmaier, P. *Macromolecules* 1990, 23, 634.